Thin Solid Films xxx (2009) xxx–xxx

Contents lists available at ScienceDirect

Thin Solid Films

journal homepage: www.elsevier.com/locate/tsf

Formation of isolated carbon nanofibers with hot-wire CVD using nanosphere lithography as catalyst patterning technique

Z.S. Houweling *, V. Verlaan, G.T. ten Grotenhuis, R.E.I. Schropp

Utrecht University, Faculty of Science, Debye Institute for Nanomaterials Science, Nanophotonics-Physics of Devices, P.O. Box 80.000, 3508 TA Utrecht, the Netherlands

ARTICLE INFO

Available online xxxx

Keywords:
Hot-wire CVD
Carbon nanotubes
Nanosphere lithography

ABSTRACT

Recently the site-density control of carbon nanotubes (CNTs) has attracted much attention as this has become critical for its many applications. To obtain an ordered array of catalyst nanoparticles with good monodispersity nanosphere lithography (NSL) is used. These nanoparticles are tested as catalyst sites in hot-wire chemical vapor deposition (HWCVD) of carbon nanostructures. Aside from using NSL also nickel (Ni) nano-islands are made by thermal annealing of a thin Ni film and tested as catalyst sites. Multiwall CNTs, isolated carbon nanofibres, and other nanostructures have been deposited using HWCVD. Tungsten filaments held at ~2000 °C are used to decompose a mixture of ammonia, methane and hydrogen. The structures have been characterized with Scanning Electron Microscopy, High Resolution Transmission Electron Microscopy, Raman spectroscopy and Rutherford Backscattering Spectroscopy.

1. Introduction

Since the key publication of Iijima on carbon nanotubes (CNTs) in 1991 [1], numerous papers about CNTs have appeared. Recently the site-density control of CNTs has attracted much attention as this has become critical for many applications such as biosensors and bioprobes [2–7] and field emission devices [8]. Since CNTs grow from catalyst particles made of transition metals, good control over the site-density of these catalyst particles is an important issue. A proven method to control the size and site-density of the catalyst particles in a cheap, fast and easy way is nanosphere lithography (NSL) [9–12]. Using NSL a self-assembled layer of colloidal spheres functions as a lithographic mask for illumination, etching or deposition. The hot-wire chemical vapor deposition (HWCVD) technique is a scalable and successful method for the growth of CNTs [13–15], this technique is to this end also used in combination with plasma enhanced (PE) CVD [16–19] and is then called HW PECVD.

2. Experimental details

The growth of carbon structures is made in a two-step process; the catalyst formation and the carbon deposition. The substrates used are 1×1 cm^2 c-Si (100) wafers. A ~200 nm thick titanium nitride (TiN_x) layer is sputtered as temperature resistant diffusion barrier layer. It prevents nickel (Ni) diffusion into the silicon wafer forming $NiSi_x$ during annealing. A chromium sulfuric acid (2–5% $Na_2Cr_2O_7$ in ~90% H_2SO_4) surface enhancement treatment was applied to promote hydrophylicity and homogenization of the surface of the substrate [20]. An ethanol solution with silica colloids with diameter D=(1400±20) nm (0.69 wt.%) is drop cast (~13 μl) onto the substrate, the ethanol evaporates while the colloids self-assemble there into a monolayer of colloids. Then a Ni overlayer is evaporated over the monolayers. The colloids are removed by sonication in ethanol and a periodic particle array (PPA) of Ni prisms remains on the sample surface. Annealing this PPA deforms the prisms into round dots.

The second step is the carbon deposition. Both the anneal step and the carbon deposition take place in a vacuum reactor called CANTOR (CArbon NanoTube reactOR). This is a combined HW PECVD reactor chamber (13.5 dm^3) with a typical base pressure of 10^{-7} mBar. In this research the plasma capability is not used and only the HWCVD mode is used. The substrates are placed on a tantalum (Ta) heating block with three built-in firerods which heat the block to a temperature of up to 950 °C. Two parallel tungsten (W) filaments (99.95% pure, 0.3 mm diameter, 10.5 cm length, placed 1 cm above the substrate) are used to decompose the source gasses methane (CH_4), ammonia (NH_3) and hydrogen (H_2). The methane acts as carbon source, the ammonia and hydrogen as etching agents. The gasses are introduced to the filaments from above. The direct current through the filaments is kept constant at 8.0 A (~2000 °C). The filaments are resistively annealed before use. A shutter is present between the substrate and the filaments to control the start and end of the deposition.

Scanning Electron Microscopy (SEM) pictures have been taken with a Philips XL machine at acceleration voltages between 5 and 30 kV. High Resolution Transmission Electron Microscopy (HRTEM) pictures have been taken with a Philips Tecnai 20 F Scripting machine at an acceleration voltage of 200 kV after scraping or sonicating off deposited material from the substrates onto a TEM grid with a thin

* Corresponding author.
E-mail address: Z.S.Houweling@uu.nl (Z.S. Houweling).

0040-6090/$ – see front matter.
doi:10.1016/j.tsf.2009.01.063

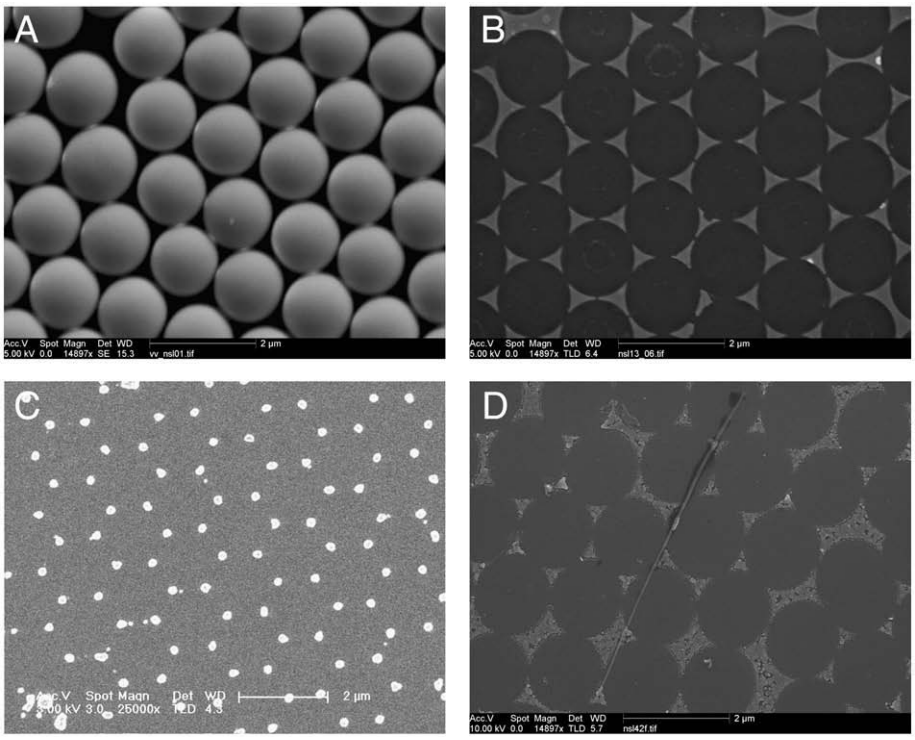

Fig. 1. (A) Silica spheres of (1400±20) nm used as a monolayer deposition mask. (B) An array of nickel prisms resides after sonication. (C) Annealing deforms the prisms into round dots. (D) A secondary electron picture of isolated carbon nanofiber formation. All pictures are made with SEM.

carbon film. Raman spectroscopy measurements have been performed with an Ar laser at an excitation wavelength of 514.5 nm with an intensity of 0.5 W. Rutherford Back Scattering (RBS) measurements have been performed with 2 MeV He^+ ions from a 3 MV single ended Van de Graaff ion accelerator.

3. Results

For the NSL method, silica (SiO_2) colloids with diameter $D=(1400\pm20)$ nm are used as a deposition mask, shown in Fig. 1(A). After evaporating a 20 nm Ni overlayer, the colloids are removed via sonication. A PPA of Ni

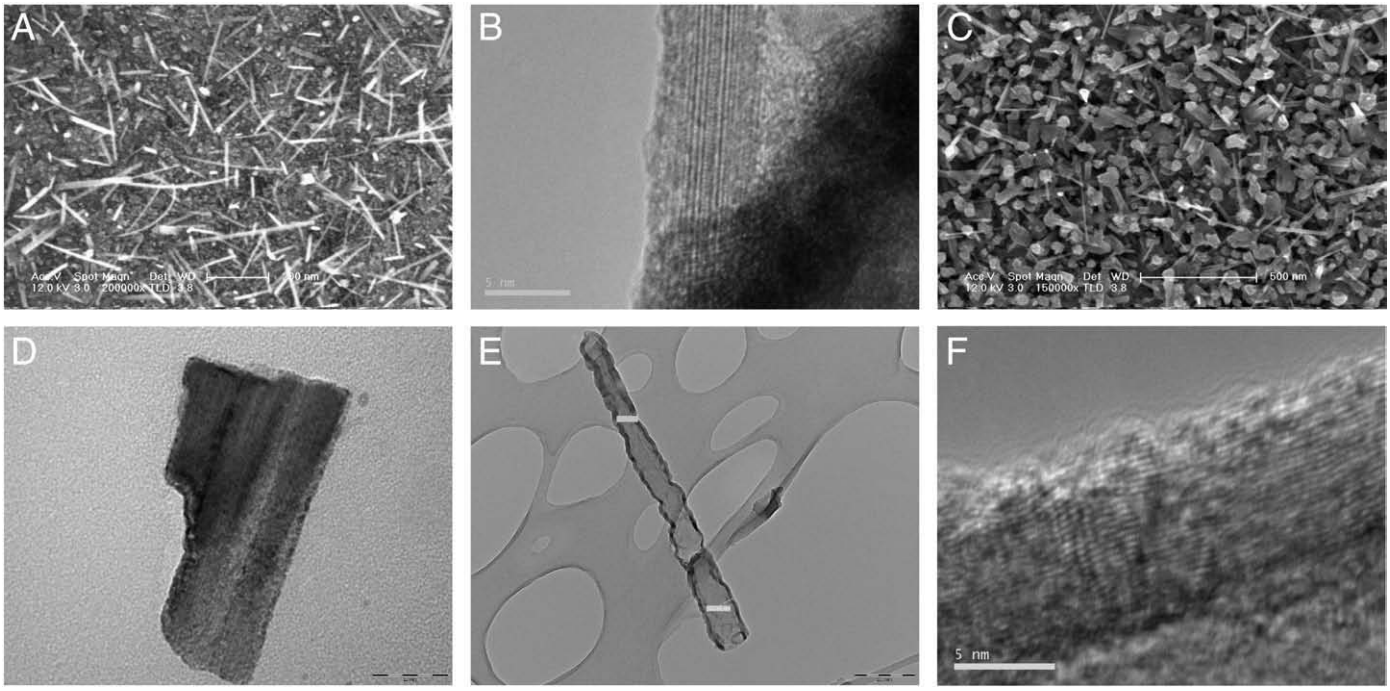

Fig. 2. (A) Nanostructures with (10±4) nm thickness and mostly shorter than 500 nm. (B) A HRTEM picture of a 6.5 nm wide nanostructure. (C) Flake-like structures. (D) A TEM picture of a flake. The scale bar is 20 nm. (E) A TEM image of a ~100 nm thick and 1.2 μm long MWCNT. The scale bar is 200 nm. (F) HRTEM picture of one of the walls of the MWCNT in Figure (E) showing graphene layers. All pictures are made with SEM or TEM.

Please cite this article as: Z.S. Houweling, et al., Thin Solid Films (2009), doi:10.1016/j.tsf.2009.01.063

prisms with height $h=20$ nm and P_{6nn} in-plane symmetry resides on the substrate, shown in Fig. 1(B). The size of the prisms is determined by SEM and amounts to $a=335$ nm, where a is defined as the perpendicular bisector of the largest inscribed equilateral triangle between three colloids. From simple geometry it follows that a should equal $(\sqrt{3}-3/2)$ D. So geometrically one expects $a=(326\pm20)$ nm, whereby the variation in a is caused by a variation in D [21]. An anneal treatment ($P=0.24$ mBar, H_2 flow = 100 sccm, $T_{filament}$ ~2000 °C, $T_{substrate}$ = 600 – 750 °C) for 30 min deforms the prisms into round dots with a diameter of $d=233\pm22$ nm, shown in Fig. 1(C).

The NSL method yields PPAs with good monodispersity and over large areas of at least 5×5 μm^2 [12,21,22]. Outside of the PPA there are areas where the colloids do not adhere well to the substrate. In these areas a continuous thin Ni film is deposited during Ni evaporation. In the thermal anneal treatment, this Ni film fragments into islands. These islands are also suitable for the growth of carbon nanofibers (CNFs) or CNTs but have no periodic pattern. The distinction we make here between tubes and fibers is merely that the first obviously have a hollow interior and the second have an internal structure.

Isolated CNFs have been made using the NSL method, a Secondary Electron (SE) image is shown in Fig. 1(D). First the substrate with a Ni PPA with $h=28$ nm was annealed for 30 min ($P=0.26$ mBar, H_2 flow = 60 sccm, $T_{filament}$ ~2000 °C, $T_{substrate}$ = 450 – 550 °C) and then the source gasses were introduced for 30 min ($P=0.26$ mBar, $CH_4/NH_3/H_2$ flow = 36/10/60 sccm, $T_{filament}$ ~2000 °C, $T_{substrate}$ = 450 – 550 °C). The Ni prisms have not deformed into dots, instead the prisms have partially cracked. This effect is likely due to a too low substrate temperature for the formation of the dots. CNFs have been found on many places on the substrate, the growth clearly starts at the Ni prisms, they are noticeably long, straight and isolated, have an approximate thickness of (116±68) nm and a length of up to ~6 μm (Fig. 1D).

Instead of using a Ni PPA, also Ni islands made by a thermal treatment were used to deposit nanostructures. First the substrate with a Ni film of 10 nm thickness was annealed for 30 min ($P=1.0$ mBar, H_2 flow = 100 sccm, $T_{filament}$ ~2000 °C, $T_{substrate}$ = 600 – 750 °C) and then the source gasses were introduced for 30 min ($P=1.0$ mBar, $CH_4/NH_3/H_2$ flow = 30/10/60 sccm, $T_{filament}$ ~2000 °C, $T_{substrate}$ = 600 – 750 °C). This time different structures formed on different places on the substrate. First, we have what appear to be thin CNFs that have diameters of (10±4) nm and lengths of up to 500 nm, an example of these fibers is shown in Fig. 2(A). A HRTEM image of such a fiber of 6.5 nm width is shown in Fig. 2(B). A fast Fourier transform (FFT) analysis is performed over an area of its surface revealing a lattice constant of 3.1 Å. Due to this lattice constant, which is close to the lattice constant of graphene (3.35 Å) and the high carbon signal in the Raman measurement (shown below) we conclude that these structures are likely to consist of carbon. Second, "flakes" were deposited, shown in Fig. 2(C). A TEM picture of a flake is shown in Fig. 2(D), the lattice constant that was determined from the HRTEM picture (not shown) is 3.2 Å. Last, multiwall CNTs were found on the TEM grid, an example is shown in Fig. 2(E). A HRTEM image of one of the walls of this MWCNT is shown in Fig. 2(F), the FFT reveals a lattice interplanar distance of 3.4 Å. The MWCNT has a length of 1.2 μm and a width of 110 nm at the base and 90 nm at the head.

A RBS measurement has been performed to identify atomic species present in the sample. The analysis is performed by simulating the elemental composition profiles in RUMP [23], which is challenging due to the roughness of the sample. The simulation reveals the c-Si substrate with the TiN_x barrier layer. We obtain the best agreement in the simulation with the measurement if we use as top layer a $W_1C_1Ni_{0.25}$ layer with a profile of C and O through it. The O/C ratio amounts to about 0.5 decreasing from surface to interface of the top layer. Since the profile of the C and O in this layer, which has a non-uniform thickness varying between 50 and 150 nm, have the same shape and the SEM pictures show nanotubes and other structures that supposedly mainly consist of C, we assume that all C and O found by RBS can be attributed to these structures. The high O content is due to an unfortunate high, though stable, base pressure in this experiment. The W found in the top layer in this RBS measurement originates from the filaments, possibly due to high base pressure and/or the aggressive nature of the atomic hydrogen during the anneal and CNT deposition. Heated W wires are known to carburize during CVD processes and form WC and W_2C phases [24–27], to determine how and in what form in our CVD process this W or WC_x is deposited in the top layer additional experiments are needed.

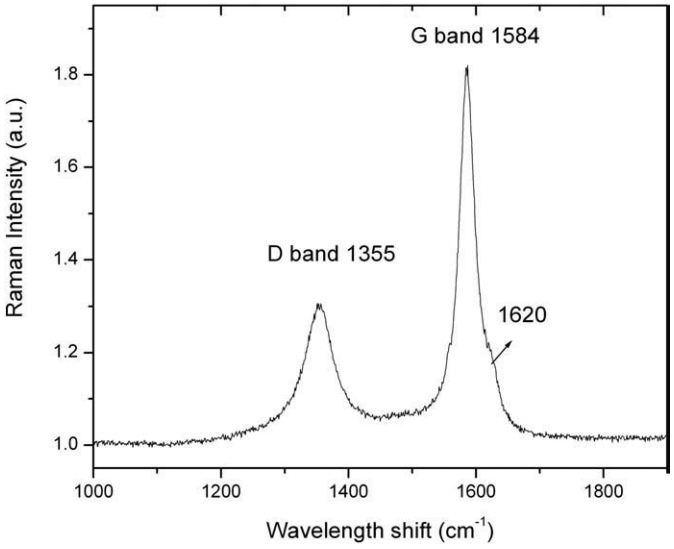

Fig. 3. Raman spectrum of the structures shown in Fig. 2.

Raman spectroscopy was performed on the substrates with these structures. The site-density of the CNTs formed was sufficient to use Raman characterization, which was not the case with the NSL substrates. The spectrum reveals a large amount of carbon present in the sample and is shown in Fig. 3. The spectrum closely resembles that of graphite [28]. Two clear modes are present at 1580 cm^{-1} and 1354 cm^{-1}, representing the G band and D band respectively. Also at 1620 cm^{-1} the D′ band can be observed. The G band is the Raman-allowed C–C phonon mode (E_{2g} band) [29]. The D′ band is due to the loss of long-range symmetry and the presence of lattice defects [30,31] and the D band at ~1350 is also a disorder-induced phonon mode. Tuinstra and Koenig [32] proposed a relationship between the intensity ratio of the D and G bands and the inverse of the in-plane coherence length (L_a), which is the mean crystallite size in graphite. This leads to the formula $L_a=C(\lambda)(I_D/I_G)^{-1}$, where $C(\lambda)$ is dependent on the laser excitation wavelength [31,33]. Here $C(\lambda)=44$ Å for $\lambda=514.5$ nm and $(I_D/I_G)^{-1}=2.02\pm0.02$, which leads to an in-plane coherence length of $L_a=89$ Å. It should be noted here that no post-deposition treatments were performed to clean or purify the substrates and nanotubes thereon.

4. Conclusions

The NSL method was used to make PPAs of Ni prisms. The prisms are tested as catalytic sites for the growth of CNFs. These CNFs have been found on many places on the substrate, the growth clearly starts at the Ni prisms, they are noticeably long, straight and isolated and have an approximate diameter of (116±68) nm and a length of up to 6 μm. Although the fibers did not grow from each individual Ni particle (prism in this case), the use of colloids with smaller diameter will yield smaller Ni dots and likely overcome this issue, hence more control can be gained. Currently we are working with colloids of 220 nm, which should yield prisms with $a=50$ nm and the results are promising.

With thin film island formation of Ni, nanostructures with a larger site-density, though randomly distributed, were made that were

characterized with RBS, Raman and HRTEM. To determine how and in what form in our CVD process the W is deposited in the top layer, additional experiments will be performed. The current results reveal that CNFs, carbon flakes consisting of highly ordered graphene planes are deposited as well as MWCNTs.

Acknowledgements

We thank Prof. John W. Geus for the assistance with the (HR)TEM imaging, Dr. Wim M. Arnold Bik for the ion beam analysis and Dr. Carlos van Kats for supplying the silica colloids. This project is undertaken with financial support from the Ministry of Economic Affairs of the Netherlands: program EOS (Subsidy Energy Research), NEO (New Energy Research).

References

[1] S. Iijima, Nature 354 (1991) 56.
[2] P.L. Flaugh, S.E. O′ Donnell, S.A. Asher, Appl. Spectrosc. 38 (1984) 847.
[3] C.H. Munro, V. Pajicini, S.V. Asher, Appl. Spectrosc. 51 (1997) 1722.
[4] J.J. Storhoff, R. Elghannian, R.C. Mucic, C.A. Mirkin, R.L. Letsinger, J. Am. Chem. Soc. 120 (1998) 1959.
[5] R. Elghanian, J.J. Storhoff, R.C. Mucic, R.L. Letsinger, C.A. Mirkin, Science 277 (1998) 1078.
[6] M. Bruchez Jr., M. Moronne, P. Gin, S. Weiss, A.P. Alivisatos, Science 281 (1998) 2013.
[7] W.C. Chan, S.M. Nie, Science 281 (1998) 2016.
[8] L. Nilsson, O. Groening, C. Emmenegger, O. Kuettel, E. Schaller, L. Schlapbach, H. Kind, J.M. Bonard, K. Kern, Appl. Phys. Lett. 76 (2000) 2071.
[9] U.C. Fischer, H.P. Zingsheim, J. Vac. Sci. Technol. 19 (1981) 881.
[10] H.W. Deckman, J.H. Dunsmuir, Appl. Phys. Lett. 41 (1982) 377.
[11] J.C. Hulteen, R.P. Van Duyne, J. Vac. Sci. Technol. 13 (1995) 1553.
[12] F. Burmeister, C. Schafle, T. Matthes, M. Bohmisch, J. Boneberg, P. Leiderer, Langmuir 13 (1997) 2983.
[13] A.C. Dillon, A.H. Mahan, J.L. Alleman, M.J. Heben, P.A. Parilla, K.M. Jones, Thin Solid Films 430 (2003) 292.
[14] K.H. Park, S. Choi, K.M. Lee, S. Lee, K.H. Koh, J. Vac. Sci. Technol., B 19 (2001) 958.
[15] T. Ono, H. Miyashita, M. Esashi, Nanotechnol 13 (2002) 62.
[16] Z.F. Ren, Z.P. Huang, J.W. Xu, J.H. Wang, P. Bush, M.P. Siegal, P.N. Provencio, Science 282 (1998) 1105.
[17] J.H. Han, W.S. Yang, J.B. Yoo, C.Y. Park, J. Appl. Phys. 88 (2000) 7363.
[18] Y. Hayashi, T. Negishi, S. Nishino, J. Vac. Sci. Technol., A 19 (2001) 1796.
[19] C.S. Cojocaru, D. Kim, D. Pribat, J.-E. Boureé, Thin Solid Films 501 (2006) 227.
[20] H.P. Jennissen, T. Zumbrink, M. Chatzinikolaidou, J. Steppuhn. Mat.-wiss. u. Werkstofftech. 30 (1999) 838.
[21] J.C. Hulteen, D.A. Treichel, M.T. Smith, M.L. Duval, T.R. Jensen, R.P. Van Duyne, J. Phys. Chem., B 103 (1999) 3854.
[22] Z.P. Huang, D.L. Carnahan, J. Rybczynski, M. Giersig, M. Sennet, D.Z. Wang, J.G. Wen, K. Kempa, Z.F. Ren, Appl. Phys. Lett. 82 (2003) 460.
[23] L.R. Doolittle, Nucl. Instrum. Methods, B 9 (31) (1985) 344.
[24] E. Zeiler, S. Schwarz, S.M. Rosiwal, R.F. Singer, Mater. Sci. Eng., A 335 (2002) 236.
[25] T.D. Moustakas, Solid State Ion 32–33 (1989) 861.
[26] H. Matsubara, T. Sakuma, J. Mater. Sci. 25 (1990) 4472.
[27] S. Okoli, R. Haubner, B. Lux, Surf. Coat. Technol. 47 (1991) 585.
[28] R.J. Nemanich, S.A. Solin, Phys. Rev., B 20 (1979) 392.
[29] R.P. Vidano, D.B. Fishbach, L.J. Willis, T.M. Loehr, Solid State Comm. 39 (1981) 341.
[30] A.C. Ferrari, J. Robertson, Phys. Rev., B 61 (2000) 14095.
[31] C. Vix-Guterl, M. Couzi, J. Dentzer, M. Trinquecoste, P. Delhaes, J. Phys. Chem., B 108 (2004) 19361.
[32] F. Tuinstra, J.L. Koenig, J. Chem. Phys. 53 (1970) 1126.
[33] M.J. Matthews, M.A. Pimenta, G. Dresselhaus, M.S. Dresselhaus, M. Endo, Phys. Rev., B 59 (1999) 6585.

Please cite this article as: Z.S. Houweling, et al., Thin Solid Films (2009), doi:10.1016/j.tsf.2009.01.063